

---

# CT-SPECT Fusion Plus Conjugate Views for Determining Dosimetry in Iodine-131-Monoclonal Antibody Therapy of Lymphoma Patients

Kenneth F. Koral, Kenneth R. Zasadny, Marc L. Kessler, Jian-Qiao Luo, Steven F. Buchbinder, Mark S. Kaminski, Isaac Francis and Richard L. Wahl

*Internal Medicine Department, Divisions of Nuclear Medicine and Hematology/Oncology, Radiation Oncology Department and Radiology Department, The University of Michigan Medical Center, Ann Arbor, Michigan*

---

A method for performing  $^{131}\text{I}$  quantitative SPECT imaging is described which uses the superimposition of markers placed on the skin to accomplish fusion of computed tomography (CT) and SPECT image sets. **Methods:** To calculate mean absorbed dose after administration of one of two  $^{131}\text{I}$ -labeled monoclonal antibodies (Mabs), the shape of the time-activity curve is measured by daily diagnostic conjugate views, the y-axis of that curve is normalized by a quantitative SPECT measurement (usually intra-therapy), and the tumor mass is deduced from a concurrent CT volume measurement. The method is applied to six B-cell non-Hodgkin's lymphoma patients. **Results:** For four tumors in three patients treated with the MB1 Mab, a correlation appears to be present between resulting mean absorbed dose and disease response. Including all dosimetric estimates for both antibodies, the range for the specific absorbed dose is within that found by others in treating B-cell lymphoma patients. Excluding a retreated anti-B1 patient, the tumor-specific absorbed dose during anti-B1 therapy is from 1.4 to 1.7 mGy/MBq. For the one anti-B1 patient, where quantitative SPECT and conjugate-view imaging was carried out back to back, the quantitative SPECT-measured activity was somewhat less for the spleen and much less for the tumor than that from conjugate views. **Conclusion:** The quantitative SPECT plus conjugate views method may be of general utility for macro-dosimetry of  $^{131}\text{I}$  therapies.

**Key Words:** radioimmunotherapy; SPECT; conjugate views; lymphoma; iodine-131

J Nucl Med 1994; 35:1714-1720

---

**P**atients with non-Hodgkins lymphoma are being treated with radioimmunotherapy (RIT) at many centers as summarized in a recent review article (1). In addition, at the University of Michigan, a Phase 1 dose-escalation study

employing the  $^{131}\text{I}$ -labeled monoclonal antibody (Mab) MB1, which binds the CD37 cell-surface antigen, has recently been completed (2). Also, a Phase 1 clinical trial using the  $^{131}\text{I}$ -labeled Mab anti-B1, which targets the CD20 cell-surface antigen, is ongoing and has produced promising preliminary results (3). Both Mabs are intravenously administered.

The possible importance of intra-therapy SPECT in achieving accurate tumor dosimetry of such patients has been indicated by a recent case study (4). The present report employs skin markers to achieve fusion of computed tomography (CT) and SPECT image sets. The resultant imaging procedure, which includes patient-specific attenuation correction, allows SPECT to become quantitative SPECT in the same sense that PET can be quantitative (relative accuracy depends on the application). A recent review (5) references the efforts of many groups in pursuit of  $^{131}\text{I}$  quantitative SPECT.

In this paper, we tabulate our resultant dosimetric values for six therapy patients: three treated with MB1 Mab and three with anti-B1. For one anti-B1 patient, we present both therapy and diagnostic quantitative SPECT results and also the effect on dosimetry of accounting for the changing volume of the tumor. No attempt is made to describe the spatial distribution of the absorbed dose within a tumor or organ, average values are presented instead.

## METHODS

### Patients and Protocol

All patients gave written informed consent for their participation. Patient characteristics are briefly summarized in Table 1. The MB1 patients were scanned after a tracer dose with a week-long series of daily conjugate views. After therapy, quantitative SPECT imaging was accomplished at a single, known time point. The anti-B1 patients underwent three separate, sequential tracer administrations. Each was evaluated with a weeklong series of daily conjugate views. The series were labeled DX1, DX2 and DX3. The difference was that DX1 was not accompanied by a cold

---

Received Oct. 21, 1993; revision accepted Apr. 18, 1994.

For correspondence and reprints contact: Kenneth F. Koral, PhD, 3480 Kresge III, University of Michigan Medical Center, 204 Zina Pitcher Place, Ann Arbor, MI 48109-0552.

**TABLE 1**  
Patient Data

Patient no.	Mab	Age (yr)	Sex	Administered activity	Cold predose	Study type
1	MB1	45	M	2.5GBq	—	Therapeutic
2	MB1	46	M	5.5	—	Therapeutic
3	MB1	67	F	3.0	—	Therapeutic
4	anti-B1	36	M	1.5	685 mg	Therapeutic
5A	anti-B1	57	M	0.19	135 mg	Diagnostic
5B	anti-B1	57	M	2.3	135 mg	Therapeutic
6	anti-B1	44	M	1.4	135 mg	Second retreatment

predose, while DX2 was accompanied by a cold predose of 135 mg of unlabeled anti-B1 and DX3 by 685 mg of unlabeled anti-B1. After DX3, the first treatment dose was administered with the “most favorable” predose. Quantitative SPECT was again accomplished at a single, known time point, usually after the therapy administration. For Patient 5, there was a quantitative SPECT study during DX2, as well as after the therapy administration. For Patient 6, the conjugate views and quantitative SPECT were for a second retreatment.

### Computed Tomography

CT was carried out with a GE9800 scanner (GE Medical Systems, Milwaukee, WI). Five ink-crossed lines were placed on the skin of the patient where transverse CT slices would intersect the tumor of interest. The locations were chosen to include a left-side, anterior, right-side and posterior reference, as well as a location similar to one of the above but displaced longitudinally about 5–10 cm. Highly x-ray absorbent, 1.5-mm diameter, lead markers (Beekley Spots™, Beekley Corp., Bristol, CT) were affixed over the intersection of the crossed lines. The patient lay supine on a flat, low-absorption table insert (Carbon-fiber, foam composite table insert, GE Medical Systems, Milwaukee WI). Slice thickness was 1 cm. Scanning was standard except that care was taken to include the skin edges and normal breathing was allowed so as to duplicate the conditions which would exist during the SPECT scan.

### Conjugate Views

The conjugate-view method employs a background subtraction and is further outlined by Koral et al. (4). It was assumed that it provided the shape of the time-activity curve in effect during dosimetry (carried out with the same cold predose in the case of anti-B1). The amplitude of the curve was normalized by the quantitative SPECT measurement. That is, activity as a percent of decay-corrected administered activity was compared at the same time after administration of the radiopharmaceutical to obtain a normalization factor; the “true” curve of activity as a percent of decay-corrected administered activity was the conjugate-view curve multiplied by normalization factor.

Phenomenologically, this normalization factor is a product of a scan factor multiplied by a physiological factor. The scan factor takes into account any difference between SPECT and conjugate-view scanning (if equally sensitive and equally accurate, it equals 1). The physiological factor takes into account any physiological differences between the scanning times, such as changed biological state of the tumor or organ or nonlinearity of uptake with the administered dose (if unchanged, it equals one). The changed biological state for anti-B1 tumors often features a mass decrease

which, by itself, causes a large decrease in the physiological component of the normalization factor. This decrease with mass occurs because both components of the normalization factor depend on activity, rather than on activity divided by mass.

### Quantitative SPECT

Quantitative SPECT with a dual-energy window tomographic acquisition was carried out with a GE 400AT camera (GE Medical Systems). The photopeak window was symmetrically set on the  $^{131}\text{I}$  peak with a 20% width and the scatter window was abutted to it on the low-energy side with a width equal in keV to that of the photopeak window. Sixty-four angles, a  $64 \times 64$  matrix and 10–30 sec per angle were used. The same table insert as used for CT was used for SPECT. Time of imaging ranged from 2 to 6 days after administration of the radiolabeled antibody.

Five SPECT markers were produced by soaking glass-fiber-paper (Silica-Gel-Impregnated Glass-Fiber Sheets, Gelman Sciences, Inc., Ann Arbor, MI) punches (diameter = 7 mm) with  $^{131}\text{I}$  radioactive solution and sealing with transparent tape. These were centered over the intersection of the ink-crossed lines.

Initial reconstruction of the SPECT projection data without attenuation correction was carried out on a Microdelta computer (Siemens Medical Systems, Hoffmann Estates, IL). Preliminary locations of the marker positions were then calculated in x- and y-axes by using profiles in the transverse images and in the z-axis by the same in coronal images. A straight-line background under the peak was assumed and a count-based centroid calculation was carried out to estimate the position.

Fusion was attained by use of a computer program which shifted, scaled and rotated the CT data in three dimensions to minimize the root mean square distance (RMSD) between corresponding marker locations (6). Here:

$$\text{RMSD} = \left[ \frac{1}{N} \sum_{i=1}^N \Delta_i^2 \right]^{1/2},$$

where N is the number of markers and

$$\Delta_i^2 = (x_{ci} - x_{si})^2 + (y_{ci} - y_{si})^2 + (z_{ci} - z_{si})^2.$$

The  $x_{ci}$ ,  $y_{ci}$  and  $z_{ci}$  are the coordinates of the  $i^{\text{th}}$  marker in the CT image and  $x_{si}$ ,  $y_{si}$  and  $z_{si}$  are those in the SPECT image.

The fusion computer program was resident on a work station. CT markers were located and SPECT marker locations refined by displaying three planes through the datasets: a cursor was moved to the visual center of intensity in all planes in an iterative, interactive mode. After superimposition, CT slices corresponding to the SPECT slices were constructed in a  $64 \times 64$  array.

The attenuation coefficient maps were derived from the fused CT slices by an energy extrapolation. Based on a two-CT-range technique introduced by Nickoloff et al. (7), our method uses three ranges:

$$\begin{aligned}\mu &= 1.131 \times 10^{-2} * \left( \frac{CT}{868.6} + 1 \right) & CT \leq -25 \\ &= 5.744 \times 10^{-6} * CT + 1.113 \times 10^{-2} & -25 < CT < 485 \\ &= 8.929 \times 10^{-3} * \left( \frac{CT}{868.6} + 1 \right) & CT \geq 485,\end{aligned}$$

where  $\mu$  is the attenuation coefficient in  $\text{mm}^{-1}$  and CT is the x-ray CT number. The middle range avoids a discontinuous change at the boundary point of the two-range method.

The dual-energy window technique was employed to correct for Compton scatter. We relied on a separate, paralyzable-model-based dead time correction for the data in each window (9). Then for each projection, the counts in the scatter window at each pixel were multiplied by a constant ( $k = 0.75$ ) and subtracted from the counts in the photopeak window for the corresponding pixel. The value of 0.75 for  $k$  came from a measurement of the activity in a large sphere located within a cylindrical phantom of a circular cross-section that contained nonradioactive water (8).

Although individual pixel values may still be changing significantly, the sum of reconstructed strength values for a region of interest (ROI) doesn't change by more than 1% after 16 iterations of the ML-EM algorithm. This number of iterations was used.

For the first MB1 patient, fusion by markers and transfer of CT Vols was not ready. To determine the edges of the tumor, a semiautomatic, second-derivative-based edge-detection program was employed. This method tended to find edges in the tails of the activity spread.

For the other patients and the elliptical-phantom measurement (see below), regions were drawn on the original CT images and transferred to the SPECT images after taking fusion into account. The tumor images were outlined by a trained radiologist (I.F.) while the organs and spheres were outlined by a nonphysician (K.F.K. or M.L.K.). These regions were comparatively tight.

The calibration factor relates activity to reconstructed strength per second of the time used in a projection. Value one was for use with volumes of interest from edge detection (only the first MB1 patient) and was  $5.06 \times 10^3 \text{ sec}^{-1} \text{ MBq}^{-1}$  ( $1.87 \times 10^2 \text{ sec}^{-1} \mu\text{Ci}^{-1}$ ). This value came from an earlier procedure (10) and depended on employing  $k = 0.75$ .

Value two was for use with transferred Vol and was obtained as follows: a cylindrical phantom of an elliptical cross-section contained three spheres with a range of volumes from 1.8 to 113  $\text{cm}^3$ . The activity concentration of  $^{131}\text{I}$  was  $3.72 \mu\text{Ci}/\text{cm}^3$  for the smallest sphere, and dropped to  $0.96 \mu\text{Ci}/\text{cm}^3$  for the largest. "Tissue" background in the water of the cylinder had a concentration of  $0.17 \mu\text{Ci}/\text{cm}^3$ . The camera calibration factor that yielded the correct activity for the largest sphere was found, assuming the same  $k$  value above. Recovery coefficients were calculated for the other two spheres.

## Dosimetry

Mean absorbed dose,  $\bar{D}$ , was computed by using the updated Medical Internal Radiation Dose (MIRD) formalism (11) contained in the computer program MIRDSE2. In terms of the administered activity,  $A_0$ , the residence time for the tumor,  $\tau$ , that for the whole body (measured by probe),  $\tau_b$ , the dose per unit

accumulated tumor activity,  $S$ , and that for cumulated whole-body activity,  $S_b$ ,

$$\bar{D} = A_0(\tau S + \tau_b S_b).$$

Howell et al. (12) have recently presented a general formalism for dosimetry with tumors that are changing over time. We approximated the absorbed fraction for beta energy,  $\phi_\beta$ , and the self-absorbed fraction for gamma energy,  $\phi_\gamma$ , as well as the total-body absorbed fraction,  $\phi_b$ , as constant with respect to time but allowed the tumor mass to be a function of time,  $m(t)$ . Then

$$S = (\Delta_\beta \phi_\beta + \Delta_\gamma \phi_\gamma)/m(t),$$

$$S_b = \Delta_\gamma \phi_b/m(t),$$

where  $\Delta_\beta$  is the mean beta energy emitted per nuclear transition and  $\Delta_\gamma$  is that for photons. The value for  $\phi_\gamma$  was kept constant at 0.03 rather than varied with tumor shape,  $\phi_\beta$  was approximated as 1, and  $\phi_b$  was calculated from total body weight by modeling the patient as an ellipsoid. For  $m(t)$  we assumed unit density and employed the CT volume:

$$m(t) = 1 * V(t).$$

The mean absorbed dose was usually calculated with  $V(t)$  equal to  $V_0$ , the volume at the time of the CT nearest in time to the SPECT. This approximation should be quite satisfactory for the MB1 patients since their tumor volumes weren't changing rapidly, and should be satisfactory for the anti-B1 patients since for them the elapsed time between CT and SPECT was kept at a minimum. For Patient 5, the usual approximation was employed and, in addition, the variation of  $V(t)$  during therapy was estimated from three CT scans: one 43 days before the therapy administration, one 20 days before, and one 6 days after. (The DX3 administration of  $^{131}\text{I}$ -labeled anti-B1 took place among these points at 42 days before the therapy administration.)

## RESULTS

### Superimposition

In the case of Patient 5 (for the therapy scan), the agreement in individual marker coordinates after fusion is mostly within 2 mm. The RMSD is 7.4 mm.

### Dead Time Correction

For Patient 4, the count rate within the scatter window ranges from 4,200 to 5,390 cps with an angle change and so the dead time correction factor is from 1.09 to 1.12. The count rate within the photopeak window ranges from 5,950 to 8,290 counts per sec and the correction factor is from 1.10 to 1.15.

### Elliptical Phantom

The camera calibration factor for transferred Vol is found to be  $2.25 \times 10^3 \text{ sec}^{-1} \text{ MBq}^{-1}$  ( $83.4 \text{ sec}^{-1} \mu\text{Ci}^{-1}$ ). The fact that this value is lower than the one determined for edge detection is consistent with the smaller number of pixels being used for the Vol. The recovery coefficients and a curve that interpolates between them are shown in Figure 1 (for other phantom results, see (13)).

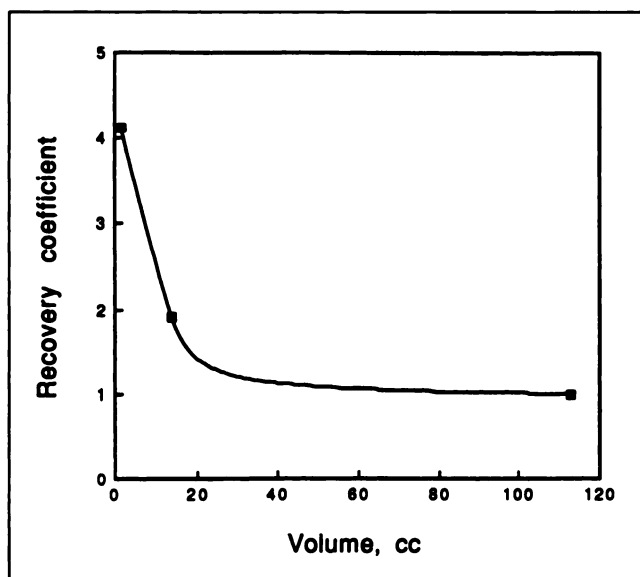


**FIGURE 1.** Plot of activity recovery coefficient versus volume from phantom experiment. Values are interpolated by a smooth curve so that a recovery coefficient could be estimated for any small tumor that has a volume greater than 1.8 cm<sup>3</sup>.

#### Quantification and Dosimetry

The time between CT and quantitative SPECT was 6 days or less (average = 2.75) for anti-B1 patients and 13 days or less (average = 5.67) for the MB1 patients.

The results for the tumors of the MB1 patients are shown in Table 2. The normalization factor ranges from considerably less than one (0.42) to considerably more than one (3.8). The largest tumor (954 cm<sup>3</sup>) has the smallest specific radiation-absorbed dose (0.35 mGy/MBq). The correlation of tumor radiation absorbed dose with disease response is shown in Table 3. The higher the calculated dose, the better the response.

The dosimetric results for the anti-B1 patients are shown in Table 4. The normalization factors are mostly less than one. For the tumors, the maximum-to-minimum ratio for specific radiation absorbed dose is only 2.4 compared to 4.4 for MB1. The tumor of the retreatment patient has the minimum value. When normal organs are included, the maximum-to-minimum ratio for specific radiation absorbed dose increases from 2.4 to 4.9.

**TABLE 2**  
Dosimetry Results for Tumors of MB1 Patients

Patient no.	Location	Volume	Normalization factor	Specific radiation absorbed dose
1	right	22.6 cm <sup>3</sup>	1.2	1.5 mGy/MBq*
	left	29.6 cm <sup>3</sup>	0.77	1.0 mGy/MBq
2		954.0 cm <sup>3</sup>	3.8	0.35 mGy/MBq
3		76.3 cm <sup>3</sup>	0.42	0.49 mGy/MBq

\*1 mGy/MBq = 1 Gy/GBq = 3.7 cGy/mCi = 3.7 rad/mCi.

**TABLE 3**  
Correlation of Absorbed Dose with Response for MB1 Patients

Patient no.	Location	Radiation absorbed dose	Response
1	right	383cGy*	Tumor shrunk 66.9%
	left	254 cGy	Tumor shrunk 17.6%
2		194 cGy	Disease was stable
3		145 cGy	Disease progressed

\*1cGy = 1 rad.

A quantitative SPECT slice through the tumor of the retreatment patient is shown in Figure 2. The uptake in the tumor for this patient is clearly greater than that in the normal left kidney or in the spleen. The calculated specific absorbed dose for the spleen is almost as large as that for the tumor, however, because of a very slow washout of activity.

For Patient 5, <sup>131</sup>I anti-B1 quantitative SPECT was carried out both for a diagnostic and also a therapy administration. A reconstructed slice for each is shown in Figure 3. Note that the patient was not quite supine on the table for the therapy scan (Fig. 3B). The tumor shrinkage shown is clearly very substantial as discussed further by Kaminski et al. (3).

For this patient's diagnostic imaging, one can simply compare results from quantitative SPECT to conjugate views at the same time for the same administration rather than for the same amount of time after a different administration. The results for the normalization factor, which is equal to the scan factor since there were no physiological changes, are as follows: For the tumor (193 cm<sup>3</sup>), the scan factor (quantitative SPECT divided by conjugate views) is small (0.22). For the larger spleen (413 cm<sup>3</sup>), it is larger (0.69), but still less than 1.

For this patient, one can also compare the specific absorbed dose from the second administration with medium predose to the first, with the scanning method unchanged, namely SPECT. The ratio of specific absorbed dose (second over first) is 2.0 as seen in Table 5. This result indicates no decrease but rather an enhancement of the ability of tumor tissue to take up and/or retain Mab as administrations proceed. The tissue volume involved was much smaller, however, and the administered activity much larger. Also, another diagnostic administration with a higher predose did intervene between the two previously compared administrations.

Finally, as far as the changing mass, the net tumor volume for the three CT times fell on a decaying-exponential curve. The r<sup>2</sup> value for the fit was 0.9965. The time for shrinkage by one-half was 16.2 days. Since there were three remnants at therapy, this net volume as a function of time was weighted by the fraction of the volume contributed by each remnant to the total at 6 days postadministration to obtain each volume variation during therapy. Using these variations, three new absorbed dose estimates

**TABLE 4**  
Dosimetry Results for Anti-B1 Patients

Patient no.	Scan	Predose	Target	Volume	Normalization factor	Specific radiation absorbed dose
4	Treatment	685 mg	Tumor	9.2 cm <sup>3</sup>	0.34	1.7 mGy/MBq
5	Second diagnostic	135 mg	Tumor	193 cm <sup>3</sup>	0.22	0.86 mGy/MBq
		135 mg	Spleen	413 cm <sup>3</sup>	0.69	0.65 mGy/MBq
5	Treatment	135 mg	Tumor	7.8 cm <sup>3</sup> *	0.018*	1.4 mGy/MBq*†
6	Second retreatment	685 mg	Tumor	85 cm <sup>3</sup>	0.19	0.70 mGy/MBq
		685 mg	Spleen	957 cm <sup>3</sup>	2.93	0.68 mGy/MBq
		685 mg	Left kidney	219 cm <sup>3</sup>	0.22	0.35 mGy/MBq

\*Average of three separate remnants with similar individual values.

†Value decreased by 10.5% since variation of volume with time is included in calculation.

were computed and averaged. The resultant average specific absorbed dose decreased by 10.5% compared to the previous value (new value equal to 1.41 mGy/MBq compared to old value of 1.58).

## DISCUSSION

Good results can be expected with our CT-SPECT methodology for several reasons:

1. The same pixels are used for the activity and for the volume measurement because Vol is transferred to quantitative SPECT from CT. This procedure avoids amplification of error when, for example, a small CT volume is erroneously coupled with a large number of SPECT pixels giving an activity-to-mass ratio (i.e., dose) which is erroneously very large.

2. The procedure gives the mean dose for the entire tumor or organ. This mean is more representative than the mean over only the hottest pixels which is obtained when the volume used in dosimetry is found from the SPECT image (the so-called "activity volume"). Unless one knows what parts of the tumor contain replicating cells, the mean dose to the whole tumor should be calculated.
3. There is less bias towards high-uptake tumors. Such a bias may occur with a reliance on SPECT edge detection: the edge cannot be reliably found for low-uptake tumors and so they are not analyzed. Our technique analyzes any tumor that can be seen on CT whether its uptake turns out to be high or low.
4. The uptake should be correctly estimated. Although the lower activity tails of the tumor are not included in the Vol, they aren't included for the spheres used in measuring the calibration factor either.

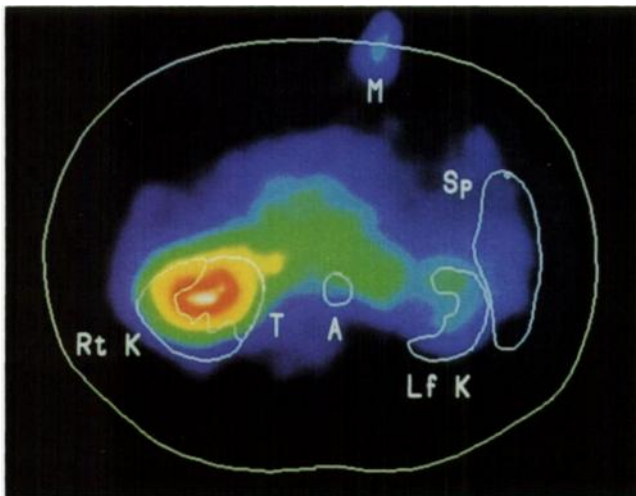


**FIGURE 2.** SPECT image of Patient 6 during retreatment. Imaging time is 47.6 hr after administration of 1.4 GBq of <sup>131</sup>I-labeled anti-B1 Mab. The tumor, T, is in intimate contact with the right kidney, Rt K. ROIs are also shown for the aorta, A, the left kidney, Lf K, the spleen, Sp, and the external body outline. A marker, M, on the skin appears at the top. The tumor-activity concentration is clearly the greatest in the image.

The contention that the quantitative SPECT-conjugate-views method is at least as accurate as other methods is supported by the good agreement with the ranges observed by others for Mab treatment of B-cell lymphoma patients as summarized in the review article by Siegel et al. (7). That is, our range for tumors with anti-B1 (0.70 to 1.7 mGy/MBq) is within their range for tumors with all antibodies (0.50–5.4 mGy/MBq). Including all our dosimetric estimates for both antibodies (covering eight tumors, two spleens and one kidney), our range of values (0.35–1.7 mGy/MBq) is within their corresponding range (0.1–5.4 mGy/MBq). Finally, for MB1 tumors only, our range (0.35–1.54 mGy/MBq) agrees with theirs (0.5–2.4 mGy/MBq) except for the lower limit which we can ascribe to the fact that our technique can handle low-uptake tumors and so we can expect to include some tumors with a low specific absorbed dose.

An indication that the method presented in this paper may be superior to that of others is that for the MB1 patients the calculated radiation absorbed dose correlates with response. Of course, the number of tumors involved,

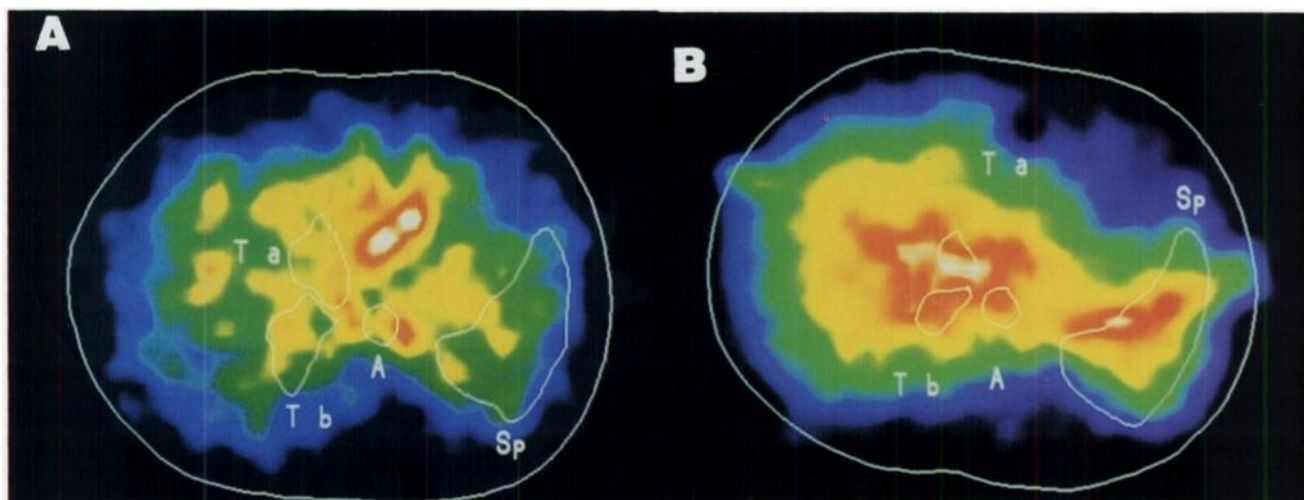


**FIGURE 3.** Comparison of diagnostic (A) and intratherapy image (B) for Patient 5. Symbols are the same as in Figure 2. The tumor at the time of the diagnostic anti-B1 imaging was large and complex. In the slice shown, it is divided into two parts, Ta and Tb, that are to the right of the liver, which itself has nonuniform uptake. The largest activity concentration for the slice is in the stomach. By the time of therapy, the tumor had shrunk into three separate remnants, two of which are shown in B. One of these remnants, Ta, the spleen and the portal vein of the liver now have the largest activity concentration.

four, is very small and the disease response is not quantitative in each case. Nevertheless, one expects that a higher absorbed dose should produce more of an effect and the calculated absorbed dose agrees with this expectation.

Obviously, direct evaluation of the quality of the activity estimates from quantitative SPECT and/or that of the macro dosimetry would be desirable. However, excisional tumor biopsy samples after tracer administration were not available to verify estimates of activity concentration and whole tumors could not be removed for macrodosimetric estimates like those possible with the methods of Erdi et al. (14) because, among other reasons, tumor response was of interest.

Some groups rely completely on conjugate views for macrodosimetry (15,16). Limited direct evidence indicating this reliance may lead to dosimetric error in some cases was found in our direct comparison of quantitative SPECT to conjugate views. The measured activity for a small tumor was much lower with quantitative SPECT than with conjugate views. This result is plausible because it is very difficult to accurately define the edges of a small tumor in a projection image. One can easily include nearby activity (in our case from the liver). If one then uses a presumably

accurate tumor volume from a CT measurement, the absorbed dose and the specific absorbed dose are both too high (since the activity was measured erroneously high). More comparisons of tumor activities from quantitative SPECT with those from conjugate views are important and of interest to us. These additional direct comparisons should further elucidate matters.

For that comparison, the measured activity with quantitative SPECT for the much larger spleen was also low, but by fractionally much less. It is more reasonable to expect that conjugate views should get the correct activity for a more isolated, larger organ like the spleen than for a small tumor. The remaining difference is perhaps due to inaccuracies in calibration factors.

The result that the second administration with a given cold predose leads to a larger specific absorbed dose than from the first administration argues for proceeding with therapy when the tumors of patients are already shrinking from diagnostic administrations because the resultant absorbed dose will be highly specific. To argue further that the therapy administration was also efficient, one would need to compare the ratio of tumor-to-blood activity for the first versus the second administration.

One difficulty with CT-SPECT fusion is that the ink marks on the skin are difficult to maintain. All inks used disappeared with time, especially if the area came into contact with soap and water. The present solution is to reapply fresh ink to fading lines. A second problem is that regional iodine contrast is present in the CT image, especially in the stomach, and is converted into regions of high attenuation coefficient in the attenuation map. During SPECT imaging at a different time, this iodine is not present. Finally, inaccuracy due to stretches and twists of the body is a concern. The fusion only allows for rigid-body chang-

**TABLE 5**  
Tumor Specific Absorbed Dose from Second Administration with Same Predose Compared to First Dose in Patient 5 with Quantitative SPECT

Administration	Activity administered	Volume	Specific absorbed dose
First	0.155 GBq	193 cm <sup>3</sup>	0.85mGy/MBq
Second	2.28 GBq	23.5 cm <sup>3</sup>	1.72mGy/MBq
Ratio*	14.6	0.12	2.0

\*Ratio is value for second divided by value for first.

es: displacement and rotation. It is possible that a warping algorithm (17,18) would produce better results.

Regardless of the problems, quantitative SPECT plus conjugate views as described may be of general utility in estimating macrodosimetry during any radiopharmaceutical therapy with  $^{131}\text{I}$ .

## ACKNOWLEDGMENTS

The authors thank Jon Johnson, RNT, Scott Moon, RNT and Shirley Zempel, RN for their technical assistance and Mrs. Patricia Haines for editorial help. The research was made possible through funding provided by grant number RO1 CA38790 (to Dr. Koral), RO1 CA 56794 (to Dr. Kaminski), and PO1 CA42768 (to Dr. Wahl) from the National Cancer Institute, National Institutes of Health, and MO1-RR00042 from the National Institutes of Health. The contents of this article are solely the responsibility of the authors and do not necessarily represent the official views of the National Cancer Institute.

## REFERENCES

1. Siegel JA, Goldenberg DM, Badger CC. Radioimmunotherapy dose estimation in patients with B-cell lymphoma. *Med Phys* 1993;20:579-582.
2. Kaminski MS, Fig LM, Zasadny KR, et al. Imaging, dosimetry and radioimmunotherapy with iodine-131-labeled anti-CD37 (MB-1) antibody in B-cell lymphoma. *J Clin Oncol* 1992;10:1696-1711.
3. Kaminski MS, Zasadny KR, Francis IR, et al. Radioimmunotherapy of B-cell lymphoma with [ $^{131}\text{I}$ ]anti-B1 (anti-CD20) antibody. *N Engl J Med* 1993;329:459-465.
4. Koral KF, Zasadny KR, Swailem FM, et al. Importance of intra-therapy single-photon emission tomographic imaging in calculating tumor dosimetry for a lymphoma patient. *Eur J Nucl Med* 1991;18:432-435.
5. Lechner PK, Koral KF, Jaszczak RJ, Green AJ, Chen GTY, Roeske JC. An overview of imaging techniques and physical aspects of treatment planning in radioimmunotherapy (RIT). *Med Phys* 1993;20:569-577.
6. Kessler ML, Pitluck S, Petti PL, Castro JR. Integration of multimodality imaging data for radiotherapy treatment planning. *Int J Radiat Oncol Biol Phys* 1991;21:1653-1667.
7. Fraass BA, McShan DL, Diaz RF, et al. Integration of magnetic resonance imaging into radiation therapy treatment planning: I. Technical considerations. *Int J Radiat Oncol Biol Phys* 1987;13:1897-1908.
8. Nickoloff EL, Perman WH, Esser PD, Bashist B, Alderson PO. Left ventricular volume: physical basis for attenuation corrections in radionuclide determinations. *Radiology* 1981;152:511-515.
9. Koral KF, Swailem FM, Clinthorne NH, Rogers WL, Tsui BMW. Dual-window Compton-scatter correction in phantoms: errors and multiplier dependence on energy [Abstract]. *J Nucl Med* 1990;31:798-799.
10. Zasadny KR, Koral KF, Swailem FM. Deadtime of an Anger camera in dual-energy-window-acquisition mode. *Med Phys* 1993;20:1115-1120.
11. Koral KF, Swailem FM, Buchbinder S, Clinthorne NH, Rogers WL, Tsui BMW. SPECT dual-energy-window Compton correction: scatter multiplier required for quantification. *J Nucl Med* 1990;31:90-98.
12. Loevinger R. MIRD primer for absorbed dose calculations. New York: The Society of Nuclear Medicine; 1988:1-21.
13. Howell RW, Narra VR, Rao DV. Absorbed dose calculations for rapidly growing tumors. *J Nucl Med* 1992;33:277-281.
14. Luo J-q. Dual-window scatter correction in quantitative single-photon-emission computed tomography. PhD dissertation, Biomedical Science, Medical Physics, Oakland University at Rochester, MI, 1993.
15. Erdi AK, Wessels BW, DeJager R, et al. Tumor activity confirmation and isodose curve display for patients receiving 1 131 - 16.88 human monoclonal antibody [Abstract]. *Antibody Immunoconj Radiopharm* 1992;5:355.
16. Eary JF, Appelbaum FL, Durack L, Brown P. Preliminary validation of opposing view method for quantitative gamma camera imaging. *Med Phys* 1989;16:382-387.
17. Eary JF, Press OW, Badger CC, et al. Imaging and treatment of B-cell lymphoma. *J Nucl Med* 1990;31:1257-1268.
18. Bookstein FL. Toward a notion of feature extraction for plane mappings. In: de Graff C, Viergever M, eds. *Proceedings of the Tenth International Conference on Information Processing in Medical Imaging*. New York: Plenum Publishing Co; 1988:23-43.
19. Bookstein FL. Principal warps: thin-plate splines and the decomposition of deformations. *IEEE Trans Pattern Analysis Machine Intelligence* 1989;11:567-585.